

Observation of Continuous Time Crystal in a Spin Maser System

Weiyu Wang,^{1,2,3} Mingjun Feng,^{1,2,3} Qianjin Ma,^{1,2,3} Zi Cai,^{4,5,*} Erwei Li,^{1,2,3} and Guobin Liu^{1,2,3,†}

¹National Time Service Center, Chinese Academy of Sciences, Xi'an 710600, China

²Key Laboratory of Time Reference and Applications,
Chinese Academy of Sciences, Xi'an 710600, China

³University of Chinese Academy of Sciences, Beijing 100049, China

⁴Wilczek Quantum Center and Key Laboratory of Artificial Structures and Quantum Control,
School of Physics and Astronomy, Shanghai Jiao Tong University, Shanghai 200240, China

⁵Shanghai Research Center for Quantum Sciences, Shanghai 201315, China

(Dated: June 24, 2024)

Pair interaction potentials between atoms in a crystal are in general non-monotonic in distance, with a local minimum whose position gives the lattice constant of the crystal. A temporal analogue of this idea of crystal formation is still pending despite intensive studies on the time crystal phase. In a hybrid spin maser system with a time delay feedback, we report the observation of a continuous time crystal induced by a retarded interaction with a characteristic time scale. This nonequilibrium phase features a self-sustained oscillation with an emergent frequency other than the intrinsic Larmor precession frequency of the spin maser system. It is shown that the amplitude of the oscillation is robust against perturbation, while its time phase randomly distributes from 0 to 2π for different realizations, a signature of spontaneous continuous time translation symmetry breaking. This CTC phase emerges only when the feedback strength exceeds a critical value, at which the system experiences a first order phase transition. Such a retarded interaction induced CTC is closer to the original idea of crystal, compared to mechanisms in other time crystal proposals.

Introduction – Crystals in nature are composed of atoms with self-organized periodic structures, which spontaneously break the continuous spatial translation symmetry into discrete ones. This idea was generalized into temporal domain[1], giving rise to an intriguing phase dubbed “time crystal”[2–4] that has attracted considerable interests in the past decade[5–20]. Time crystals can be classified as discrete or continuous depending on whether the broken translation symmetry is discrete or continuous. The continuous time crystal (CTC) has been observed in various systems including superfluid ³He[21], atom-cavity[22], semiconductor[23] and exciton-polariton system[24], while the underlying mechanism behind most CTCs to date is the limit cycle: an asymptotic periodic solution of nonlinear differential equations corresponding to a closed phase space trajectory robust against perturbations. Searching for CTC beyond this limit cycle scenario remains challenging for both theorists and experimentalists.

The interaction potential in a crystal is in general non-monotonic in distance, with a potential minimum whose position provides a key ingredient of a crystal: the lattice constant. A temporal analogue of this picture requires a retarded interaction which is nonlocal in time and with a characteristic time scale akin to the lattice constant. Compared to the widely existed nonlocal interactions in space, time-delay interactions are much rarer in nature: they usually appear as effective interactions induced by natural environments or artificial feedback protocols. Feedback is procedure of modifying system parameters according to the measurement outcomes, which plays an important role in physics and engineering[25–34]. In most realistic systems, feedback is not instantane-

ous but accompanied by a time delay with a characteristic time scale, thus can be considered as a source of retarded interaction. Take a spin system for an example, if the magnetization of spins are continuously measured, and fed back into the system Hamiltonian with a time delay τ , thus the dynamics of the spin at time t depends on the spin magnetization in earlier time $(t - \tau)$. As a consequence, such a feedback procedure actually builds up an effective retarded interaction with a characteristic time scale (τ) between spins at different times.

Motivated by this analogue, in this study, we report an experimental observation of a CTC phase in a Rb-Xe hybrid spin maser system with a feedback induced retarded interaction. Spin maser is a self-driven oscillating atomic system[35–37], where a phase coherent feedback is used to maintain the persistent spin oscillation of macroscopic ensemble of atoms and balance the spin depolarization or decoherence. The spin maser is not only with practical significance in geomagnetic measurements[38, 39] and magnetic navigation[40], but also of fundamental interest in the searching for permanent electric dipole moment [41–43] and spin-dependent exotic interactions [44]. Unlike the conventional spin maser system where the feedback is used to amplify the signal and maintain spin precession with the Larmor frequency, the feedback in our system with a time delay leads to an effective retarded interaction. This retarded interaction is responsible for a self-sustained oscillation in a macroscopic ensemble with an emergent frequency different from the intrinsic Larmor frequency, but is crucially determined by the phase lag of the time delay feedback. The experimental evidences of the two ingredients of CTC: its robustness and spontaneous symmetry breaking, have been demonstrated and

it is shown that such a CTC phase only emerges when the feedback strength exceeds a critical value.

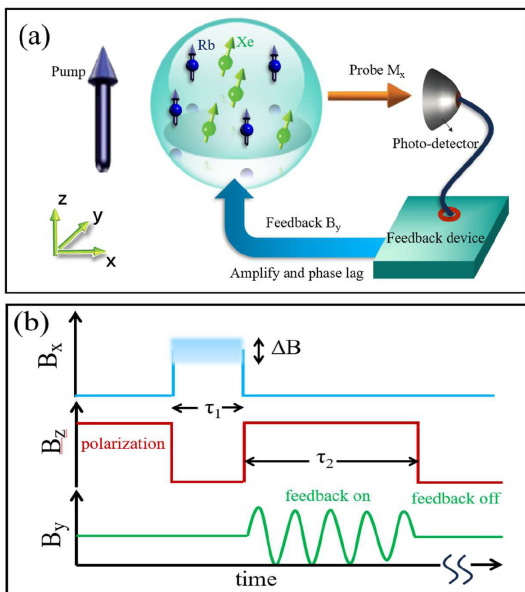


FIG. 1. Schematic drawing of the experimental setup and time sequence protocol. (a) The vacuum glass cell contains several torrs of ^{129}Xe and a small droplet of ^{87}Rb atoms. The wavelengths of the pump and probe lasers are 795 nm and 780 nm, corresponding to the D_1 and D_2 lines of ^{87}Rb respectively. (b) In a single experiment realization, spins are first polarized by optical pumping for 40 ~ 60 seconds. Preliminarily, the benchmarks are set to $I_{x,0} = 1000 \mu\text{A}$ (current-to-magnetic-field conversion coefficient $C_{B/I} \sim 1.55 \text{ mG/mA}$) and $\tau_{1,0} = 300 \text{ ms}$. The feedback-off (or depolarization) period lasts for 40 ~ 60 seconds, same as the polarization period.

Experimental setup – To observe the CTC in a spin maser system, we prepare a thermal ensemble of Rb- ^{129}Xe hybrid atomic spins, as illustrated in Fig.1(a). As the first step, a hot ($\sim 120 \text{ }^\circ\text{C}$) gaseous Rb-Xe vapor (containing a droplet of natural abundance Rb, 5 torr of isotope enriched ^{129}Xe and 50 torr of buffer gas N_2) is pumped with a resonant laser along the z axis, Rb spins are first polarized and subsequently, this polarization is transferred to Xe spins via rapid spin-exchange collision. Secondly, the Xe spins precess around a dc magnetic field B_z along the z axis. The precession is followed by Rb spins and read out by an off-resonant laser with an optical polarimeter protocol in the x axis [45]. At last, the photodetector signal is processed by an electric circuit, which can amplify the ac signal with a tunable phase lag. After that, the signal is fed back via a magnetic coil along the y axis, which, in turn drives the Xe spins coherently.

For a single experimental realization as depicted in Fig.1(b), we prepare the initial state by first utilizing 795-nm pump laser in the z axis with power of approximately 40 mW, which polarizes the spins in the system along z -direction, then imposing a magnetic pulse along

x -direction (B_x) with a short duration τ_1 on the ensemble to rotate the spin around the x -direction by an angle $\alpha = \gamma B_x \tau_1$, with γ being the magnetogyric ratio.

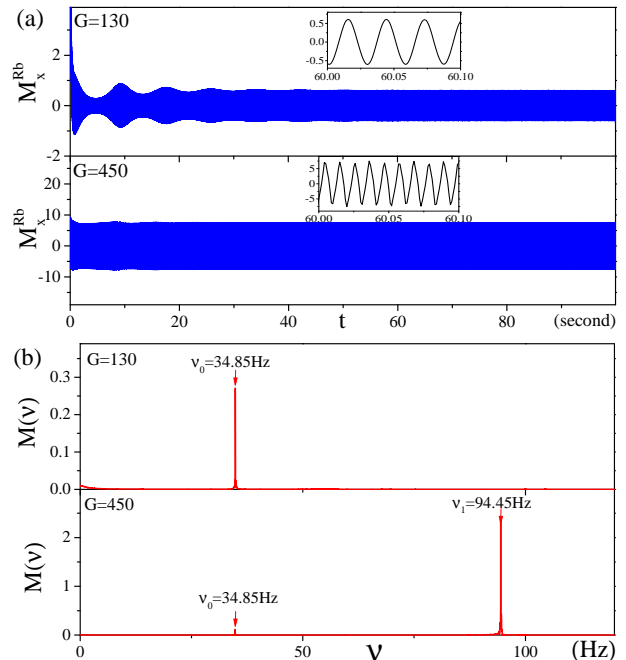


FIG. 2. (a) The dynamics of magnetization of Rb along x -direction (M_x^{Rb}) in the presence of weak (upper panel with $G = 130$) and strong (lower panel with $G = 450$) feedback (the insets zoom out the time axis of the figures) and (b) the corresponding Fourier spectra in frequency domain. The phase lag is fixed as $\theta = \pi/2$.

After preparation of such a polarized state, we apply a magnetic field along the z axis (B_z) with a duration $\tau_2 \gg \tau_1$, and at the same time, continuously monitor the polarization along x -direction of the Rb atomic spins. This signal is transmitted to the feedback device, where the original signal from the vapor cell is processed then fed back to the system parameter via the B_y coil. Such a feedback system is devised to produce a transverse magnetic field $\mathbf{B}_f = (0, B_y^f, 0)$ in response to a measured polarization M_x^{Rb} as:

$$B_y^f(t) = \frac{C_y G}{R} V_{pd} \left(t - \frac{\theta}{\nu_0} \right) \quad (1)$$

where R is the impedance of load (including a resistor and an inductive magnetic coil), G represents the electric circuit gain factor and C_y ($\sim 2 \text{ mG/mA}$) is the coil coefficient of the B_y field. V_{pd} is photodetector output voltage, which is proportional to M_x^{Rb} . ν_0 is the intrinsic Larmor frequency of the spin maser system which is proportional to B_z . θ is the phase lag between the feedback field B_y^f and the measured polarization M_x^{Rb} , which is proportional to the delay time in the feedback process. The parameters in our feedback system is highly tunable: the amplifier gain factor G ranges from 0 to 640

and phase lag θ is from $\pi/9$ to $5\pi/6$. The probe laser power is kept down to $\simeq 1$ mW to prevent signal saturation in the photodetector.

In the final step of the experiment realization, the feedback and the polarized magnetic field (B_z) are turned off, thus the system is depolarized and return to the initial state, from which we can start over again to perform another experimental realization.

Experimental verification of CTC – Fig. 2(a) shows typical real-time signals of spin maser system ($\sim M_x^{\text{Rb}}$) with weak and strong feedback strengths respectively. Their corresponding Fourier spectra are plotted in Fig. 2 (b). For a weak feedback (*e.g.* $G = 130$), one can observe a sharp peak at ν_0 in the Fourier spectrum, corresponding to the Larmor frequency of precession around the polarized field B_z ($\nu_0 = \gamma_{\text{Xe}} B_z \simeq 35$ Hz with $B_z \simeq 30$ mG and $\gamma_{\text{Xe}} = -2\pi \times 1.178$ rad \cdot kHz/G is the magnetogyric ratio for Xe spins[37, 44, 46]). So in this case, the feedback is implemented to compensate for the energy loss and the spin depolarization, and sustain the intrinsic Larmor precession of the spin maser system. However, it doesn't induce new signal with other frequency.

In the presence of a strong feedback (*e.g.* $G = 450$), however, the situation is different. In addition to the original peak at ν_0 , a stronger signal suddenly emerges at $\nu_1 \simeq 94$ Hz, which indicates a self-sustained oscillation with an emergent frequency independent of the intrinsic Larmor frequency of the spin maser system, thus provides an evidence of CTC. When the feedback is turned off, the ν_1 signal disappears immediately while the ν_0 signal decays exponentially as in the free induction decay mode (non-maser mode).

One of the ingredient of CTC is its robustness against perturbation. To demonstrate this point, we exert a perturbation ΔB_x on in the initialization pulse height B_x , thus the rotating angle in the initial state becomes:

$$\alpha = (1 - \varepsilon)\gamma B_x \tau_1 \quad (2)$$

where the dimensionless parameter $\varepsilon = \Delta B_x / B_x$. As shown in Fig. 3 (a) and (b), after the initial transient time, the amplitude of the oscillation for systems with different ε agree with each other within the error bar (see Fig. 3 b), while their time phases are different.

The CTC is also associated with a spontaneous continuous time translation symmetry breaking, which means that the time phases of the oscillations in independent experimental realizations take random values with an uniform distribution between 0 and 2π . In contrast, the relative time phases in oscillations induced by polarized magnetic field (B_z) takes a fixed value depending on the initial polarization. To verify this point experimentally, we fix $G = 640$ and $\theta = \pi/2$ in the strong feedback regime, repeat the experimental realization for \mathcal{N} times ($\mathcal{N} = 100$), and extract the relative phase from the oscillation in each experimental realization. These relative phases are plotted as the axial angle in Fig. 3(c), which

exhibits a random distribution between 0 and 2π , agreeing with the criteria of spontaneous continuous symmetry breaking. As a comparison, we also measure the relative phases without feedback ($G = 0$), whose distribution is within a narrow regime as depicted in Fig. 3 (d), indicating the absence of spontaneous symmetry breaking in this case.

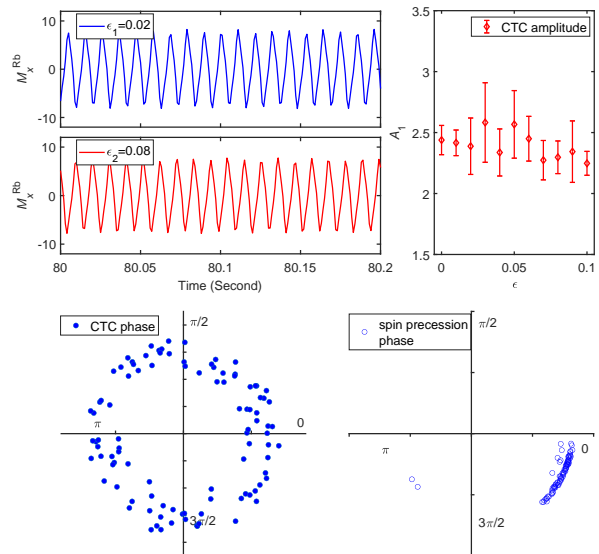


FIG. 3. (a) The dynamics of M_x^{Rb} starting from two different initial states characterized by the parameter ε . (b) The amplitude of the CTC oscillation as a function of ε characterizing different initial states. (c) and (d) The distribution of the time phases (the axial angles of the solid and empty dots) in 100 physical realizations of (c) the CTC oscillation in the case with strong feedback $G = 640$ and (d) the intrinsic Larmor precession in the system without feedback ($G = 0$). The phase lag is fixed as $\theta = \pi/2$.

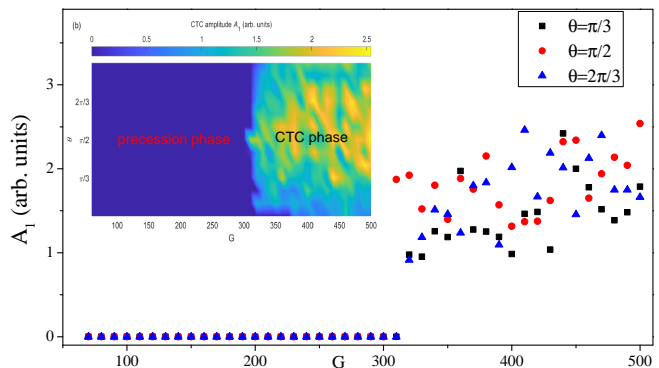


FIG. 4. The amplitude of the CTC oscillation A_1 as a function of G in the presence of different θ , a 1st order phase transition occurs at $G \simeq 300$. The inset indicates the amplitude as a function of G and θ and the global phase diagram.

Dynamical phase transition and the phase diagram –

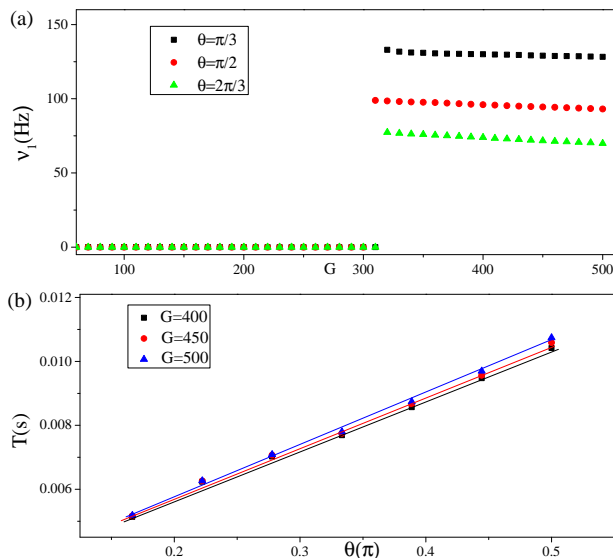


FIG. 5. (a) The frequency of the CTC oscillation (ν_1) as a function of G in the presence of different θ . (b) The period of CTC $T = 1/\nu_1$ as a function of the phase lag θ for different G .

After comparing the different dynamical phases in weak and strong feedback regime, we now focus on the phase transition between them as well as the phase diagram in terms of the two control parameters of our feedback system, the feedback strength G and the phase lag θ . Since the presence of CTC is accompanied by emergence of the peak at ν_1 , we choose the height of the ν_1 peak in the Fourier spectrum A_1 as an order parameter to characterize the CTC phase. For different θ , A_1 as a function of G is plotted in Fig.4, from which we can find a sudden jump from zero to a finite value occurs at a critical value of $G = G_c$, indicating that the system experiences a discontinuous phase transition. We notice that at the critical point, the corresponding feedback magnetic field $B_f^y \simeq B_z$, indicating that the CTC emerges when the feedback field surpasses the original magnetic field. The phase diagram in terms of G and θ is also plotted in the inset of Fig.4, which indicates that in a large regime of θ ($\pi/3 < \theta < 5\pi/6$), the corresponding G_c barely depends on θ .

Besides the amplitude, the frequency of the emergent self-sustained oscillation (ν_1) is another important feature to characterize CTC, and we will study the dependence of ν_1 on the control parameters in our feedback system. ν_1 as a function of G for different θ is plotted in Fig.5 (a), from which we can see that once the system enters the CTC phase, ν_1 barely depends on G , but is crucially determined by θ .

As we stated above, the feedback procedure in our setup leads to an effective retarded interaction with a characteristic time scale (the delay time τ), which is responsible for the emergent period of the CTC phase. To

figure out the relationship between the delay time (proportional to the phase lag θ in Eq.(1)) and the CTC period $T = 2\pi/\nu_1$, we plot T as a function of θ for different G in Fig.5 (b), which approximately exhibit linear relations, whose slopes slightly depend on the value of G . This result shows that the “lattice constant” of the CTC is indeed proportional to the characteristic time scale in the feedback-induced retarded interaction.

Discussion – Finally, we add some remarks about the spontaneous time translation symmetry breaking, which is usually referred to persistent oscillations emerging from systems without explicit time-dependence. Even though our system is “time dependent”, the time dependence enters our system through the relative time difference (delay time) in terms of two-body interactions which are still translational invariant, in contrast to the Floquet engineering whose time-dependence is explicitly through overall time. As a consequence, such a retarded interaction induced CTC is closer to the original idea of crystal, compared to those time crystal mechanisms based on nonlinearity, which comes from either a mean-field [47] or a coarse-grained treatment [48, 49] of the interaction. Another evidence of the spontaneous symmetry breaking in our system is that the CTC phase emerges only when the feedback strength exceeds a critical value, a reminiscence of certain solid state systems where the charge density wave order can only emerge for a sufficiently strong interaction.

Conclusion and outlook– In conclusion, in a Rb-Xe hybrid spin maser system with time-delay feedback, we observed a new type of continuous time crystal, which straightforwardly generalizes the concept of crystal into time domain. This result demonstrates that the feedback, besides being a signal amplifier and stabilizer, can also lead to intriguing non-equilibrium phases of matter when the retardation effect is included. Apart from its fundamental interest, the potential technological application of this retardation-induced CTC phase in time metrology and precision measurement can also be envisioned.

Acknowledgement– GL acknowledges the support by Chinese Academy of Sciences (Grant No. E209YC1101). ZC is supported by the National Key Research and Development Program of China (Grant No. 2020YFA0309000), NSFC of China (Grant No.12174251), Natural Science Foundation of Shanghai (Grant No.22ZR142830), Shanghai Municipal Science and Technology Major Project (Grant No.2019SHZDZX01)

* zcai@sjtu.edu.cn

† liuguobin@ntsc.ac.cn

[1] F. Wilczek, Phys. Rev. Lett. **109**, 160401 (2012).

- [2] K. Sacha and J. Zakrzewski, Reports on Progress in Physics **81**, 016401 (2018).
- [3] D. V. Else, C. Monroe, C. Nayak, and N. Y. Yao, Annual Review of Condensed Matter Physics **11**, 467 (2020).
- [4] M. P. Zaletel, M. Lukin, C. Monroe, C. Nayak, F. Wilczek, and N. Y. Yao, Rev. Mod. Phys. **95**, 031001 (2023).
- [5] P. Bruno, Phys. Rev. Lett. **111**, 070402 (2013).
- [6] H. Watanabe and M. Oshikawa, Phys. Rev. Lett. **114**, 251603 (2015).
- [7] K. Sacha, Phys. Rev. A **91**, 033617 (2015).
- [8] D. V. Else, B. Bauer, and C. Nayak, Phys. Rev. Lett. **117**, 090402 (2016).
- [9] V. Khemani, A. Lazarides, R. Moessner, and S. L. Sondhi, Phys. Rev. Lett. **116**, 250401 (2016).
- [10] N. Y. Yao, A. C. Potter, I.-D. Potirniche, and A. Vishwanath, Phys. Rev. Lett. **118**, 030401 (2017).
- [11] S. Choi, J. Choi, R. Landig, G. Kucsko, H. Zhou, J. Isoya, F. Jelezko, S. Onoda, H. Sumiya, V. Khemani, et al., Nature **543**, 221 (2017).
- [12] J. Zhang, P. W. Hess, A. Kyprianidis, P. Becker, A. Lee, J. Smith, G. Pagano, I. D. Potirniche, A. C. Potter, A. Vishwanath, et al., Nature **543**, 217 (2017).
- [13] Z. Cai, Y. Huang, and W. V. Liu, Chin.Phys.Lett. **37**, 050503 (2020).
- [14] N. Träger, P. Gruszecki, F. Lisiecki, F. Groß, J. Förster, M. Weigand, H. Głowiński, P. Kuświk, J. Dubowik, G. Schütz, et al., Phys. Rev. Lett. **126**, 057201 (2021).
- [15] X. Yang and Z. Cai, Phys. Rev. Lett. **126**, 020602 (2021).
- [16] J. N. Stehouwer, H. T. C. Stoof, J. Smits, and P. van der Straten, Phys. Rev. A **104**, 043324 (2021).
- [17] A. Kyprianidis, F. Machado, W. Morong, P. Becker, K. S. Collins, D. V. Else, L. Feng, P. W. Hess, C. Nayak, G. Pagano, et al., Science **372**, 1192 (2021).
- [18] X. Mi, M. Ippoliti, C. Quintana, A. Greene, Z. Chen, J. Gross, F. Arute, K. Arya, J. Atalaya, R. Babbush, et al., Nature **601**, 531 (2022).
- [19] P. Frey and S. Rachel, Sci.Adv. **8**, 7652 (2022).
- [20] J. Randall, C. E. Bradley, F. van der Gronden, V. A. Galicia, M. H. Abobeih, M. Markham, D. J. Twitchen, F. Machado, N. Y. Yao, and T. H. Taminiau, Science **374**, 1474 (2021).
- [21] S. Autti, V. B. Eltsov, and G. E. Volovik, Phys. Rev. Lett. **120**, 215301 (2018).
- [22] P. Kongkhambut, J. Skulte, L. Mathey, J. G. Cosme, A. Hemmerich, and H. Kessler, Science **377**, 670 (2022).
- [23] A. Greilich, N. E. Kopteva, A. N. Kamenskii, P. S. Sokolov, V. L. Korenev, and M. Bayer, Nature Physics **20**, 631 (2024).
- [24] I. Carraro-Haddad, D. L. Chafatinos, A. S. Kuznetsov, I. A. Papuccio-Fernandez, A. A. Reynoso, A. Bruchhausen, K. Biermann, P. V. Santos, G. Usaj, and A. Fainstein, Science **384**, 995 (2024).
- [25] A. B. Magann, K. M. Rudinger, M. D. Grace, and M. Sarovar, Phys. Rev. Lett. **129**, 250502 (2022).
- [26] E. P. Yamaguchi, H. M. Hurst, and I. B. Spielman, Phys. Rev. A **107**, 063306 (2023).
- [27] L.-N. Wu and A. Eckardt, Phys. Rev. Research **4**, L022045 (2022).
- [28] B. M. Terhal, Rev. Mod. Phys. **87**, 307 (2015).
- [29] H. M. Hurst, S. Guo, and I. B. Spielman, Phys. Rev. Research **2**, 043325 (2020).
- [30] S. Lloyd and J.-J. E. Slotine, Phys. Rev. A **62**, 012307 (2000).
- [31] M. H. Muñoz Arias, P. M. Poggi, P. S. Jessen, and I. H. Deutsch, Phys. Rev. Lett. **124**, 110503 (2020).
- [32] M. McGinley, S. Roy, and S. A. Parameswaran, Phys. Rev. Lett. **129**, 090404 (2022).
- [33] D. A. Ivanov, T. Y. Ivanova, S. F. Caballero-Benitez, and I. B. Mekhov, Phys. Rev. Lett. **124**, 010603 (2020).
- [34] S. Wu and Z. Cai, Science Bulletin **68**, 2010 (2023).
- [35] A. L. Bloom, Appl. Opt. **1**, 61 (1962).
- [36] T. E. Chupp, R. J. Hoare, R. L. Walsworth, and B. Wu, Phys. Rev. Lett. **72**, 2363 (1994).
- [37] T. Sato, Y. Ichikawa, S. Kojima, C. Funayama, S. Tanaka, T. Inoue, A. Uchiyama, A. Gladkov, A. Takamine, Y. Sakamoto, et al., Physics Letters A **382**, 588 (2018).
- [38] P. Dyal, J. Johnson, R. T., and J. C. Giles, Review of Scientific Instruments **40**, 601 (1969), ISSN 0034-6748.
- [39] T. Kubo, Appl. Opt. **11**, 1521 (1972).
- [40] A. J. Canciani, IEEE Transactions on Aerospace and Electronic Systems **58**, 420 (2022).
- [41] P. G. Harris, C. A. Baker, K. Green, P. Iaydjiev, S. Ivanov, D. J. R. May, J. M. Pendlebury, D. Shiers, K. F. Smith, M. van der Grinten, et al., Phys. Rev. Lett. **82**, 904 (1999).
- [42] M. A. Rosenberry and T. E. Chupp, Phys. Rev. Lett. **86**, 22 (2001).
- [43] M. V. Romalis, W. C. Griffith, J. P. Jacobs, and E. N. Fortson, Phys. Rev. Lett. **86**, 2505 (2001).
- [44] M. Jiang, H. Su, Z. Wu, X. Peng, and D. Budker, Science Advances **7**, eabe0719 (2021).
- [45] D. Budker, W. Gawlik, D. F. Kimball, S. M. Rochester, V. V. Yashchuk, and A. Weis, Rev. Mod. Phys. **74**, 1153 (2002).
- [46] E. Li, Q. Ma, G. Liu, P. Yun, and S. Zhang, Phys. Rev. Appl. **20**, 014029 (2023).
- [47] H. P. Ojeda Collado, G. Usaj, C. A. Balseiro, D. H. Zanette, and J. Lorenzana, Phys. Rev. Res. **3**, L042023 (2021).
- [48] Z. Gong, R. Hamazaki, and M. Ueda, Phys. Rev. Lett. **120**, 040404 (2018).
- [49] P. Yang, M. Baggioli, Z. Cai, Y. Tian, and H. Zhang, Phys. Rev. Lett. **131**, 221601 (2023).